DEVELOPMENT AND INTEGRATION OF A LOW COST, HIGH VOLTAGE POWER SUPPLY INTO A THIN FILM DEPOSITION SYSTEM

By

Andrew C. Redman

A thesis submitted in partial fulfillment of the
requirements for the degree of

Bachelor of Science

Houghton College

May 2017

Signature of Author……..
Department of Physics
May 19, 2017

……..
Dr. Brandon Hoffman
Associate Professor of Physics
Research Supervisor

……..
Dr. Kurt Aikens
Assistant Professor of Physics

DEVELOPMENT AND INTEGRATION OF A LOW COST,
HIGH VOLTAGE POWER SUPPLY INTO A THIN FILM DEPOSITION SYSTEM

By

Andrew C. Redman

Submitted to the Department of Physics
on May 11, 2017 in partial fulfillment of the
requirement for the degree of
Bachelor of Science

Abstract

An apparatus was constructed to systematically deposit thin metal films using thermionic emission. Rough vacuum is reached by a rotary pump and a turbomolecular pump is used to lower the pressure to $3x10^{-7}$ Torr. Thermionic emission is achieved by passing current through a tungsten filament floating at a -3 kV relative to the target material. Two 2 kV transformers designed for use in a microwave oven were used to create a safety interlocked, low cost, high voltage power supply capable of supplying 0.1 A peak current at 3 kV. Tests are being conducted to determine the consistency of the power supply and create a repeatable process for depositing a thin film. While deposition has not yet been achieved, the power supply is capable of delivering enough power to facilitate deposition. Power factor corrections to the power supply as well as future work are discussed.

Thesis Supervisor: Dr. Brandon Hoffman
Title: Associate Professor of Physics

TABLE OF CONTENTS

TABLE OF FIGURES

Chapter 1

HISTORY AND THEORY

1.1. Introduction

Thin films are currently being used in the development of semiconductors and transistors, which play a key role in the design of microcontroller and computer chips. Understanding the way thin films respond to thermal and mechanical stresses will give us insight into the failure rate of these chips. Houghton College is interested in studying the makeup of silver thin films, but currently relies on external research and commercial groups to supply silver thin films for testing. For this reason, the physics department at Houghton College is working to develop a thin film deposition system. Depositing a thin film requires the use of both low-pressure equipment and high-voltage electronics. Due to the high cost of commercial high voltage power supplies, a power supply was fabricated from available consumer-grade parts.

1.2. Background

1.2.1. Vacuum Science

Experimental vacuum science began in the 17th century [1]. At the time, much of the theory behind these experiments was misguided. Experiments focused on understanding the nature of the empty space left behind after a volume was evacuated. Many common phenomena now known to be caused by an external pressure, such as the rise of water in a pump, were attributed to nature's inherent avoidance of a perfect vacuum. Experiments by Torricelli and Guericke were integral in laying a foundation for the modern vacuum science.

Working off of an observation made by his mentor, Galilei, that water could not be lifted indefinitely by a hand pump, Torricelli began investigating how high mercury could be raised [2]. Torricelli hypothesized that the height of the mercury would be related to its density. Torricelli upended a glass tube of mercury, open at one end, into an open container of mercury. The result was an empty area at the top of the tube larger than the one created when performing the experiment with water. Torricelli observed that the height of the

mercury was related to the atmospheric pressure. Changes in weather and altitude affected the height of the mercury.

This device became Torricelli's famous mercury barometer. The design is shown in Figure 1. Gravity exerts a downward force on the mercury, causing it to fall down the tube [2]. This downward force is counteracted by an upward force caused by the atmospheric pressure on the mercury in the open container. As the atmospheric pressure varies, the level of the mercury in the glass tube varies, allowing the pressure to be inferred. As there is nothing to fill the area above the mercury, the area is at a low pressure. As the mercury falls farther down the tube, less mercury is in the tube and the gravitational force decreases. Once the magnitude of this force is equal to the force exerted by the atmosphere on the surface of the mercury, the mercury ceases to fall through the tube. As the atmospheric pressure changes, the level of the mercury in the tube rises and falls to reflect this change. This device was the inspiration for a continuous vacuum pump later designed by Sprengel [3]. However more advanced experiments could not be considered until pump technology advanced.

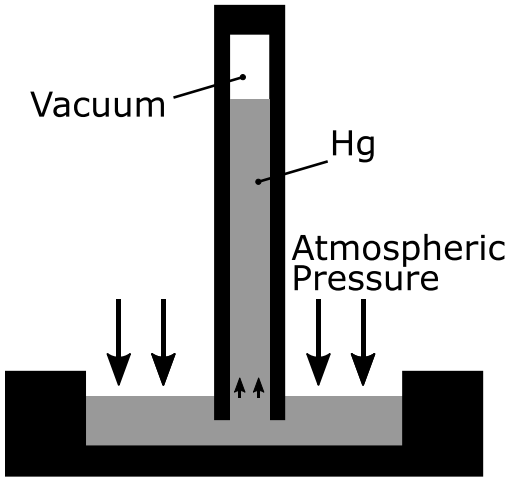

Figure 1. Diagram of a Toricelli mercury barometer. A glass tube is filled with mercury and inverted in a plate of mercury. Gravity draws the mercury down the tube creating a vacuum at the top. As atmospheric pressure changes, the force applied to the mercury in the plate fluctuates causing the mercury to rise and fall in the tube.

In the middle of the 17th century, Otto Von Guericke created a vacuum pump using a piston and two valves [4], as shown in Figure 2. Von Guericke was the first to use a vacuum pump

to continuously evacuate air from a rigid container. As the piston is drawn upwards, external air pressure holds the outer valve shut while the inner valve is allowed to open, drawing air into the piston cylinder. When the piston is compressed, the air within the cylinder is compressed, closing the inner valve, and forcing air through the outer valve. Von Guericke performed experiments demonstrating the power required to open a container once it had been sealed and evacuated. Groups of strong men or teams of horses were tasked with separating two spherical halves of a large container held shut only by atmospheric pressure.

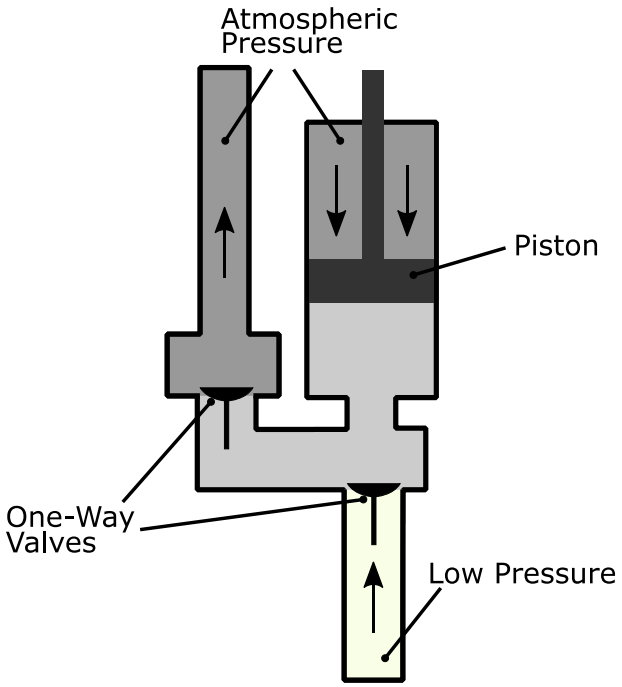

Figure 2. Piston pump design. Otto Von Guericke's original design for a piston pump utilized two strokes. The first stroke drew fluid from the chamber, while the second stroke ejected the fluid from the apparatus. Valves are in place to prevent the fluid from flowing backwards.

In 1851, an improved version of Otto Von Guericke's pump was used to evacuate a chamber to a record breaking 0.5 Torr [5]. The development of vacuum technology expanded rapidly as it began to see usage in an industrial setting. In 1905 the first rotary pump was invented [6]. This pump was capable of lowering the pressure to 1 μTorr with backing pressure from another pump. Between the years 1850 and 1900 the importance of clean equipment made

of low outgassing material was recognized and the lowest pressure achieved dropped from 10 Torr to $1x10^{-5}$ Torr [7].

Modern manufacturing technology has allowed the development of a variety of new pumps. For example, a rotary vane vacuum pump removes air from a chamber using a spring-loaded blade, as shown in Figure 3. Two sliding arms ensure that the inlet and exhaust are always sealed.

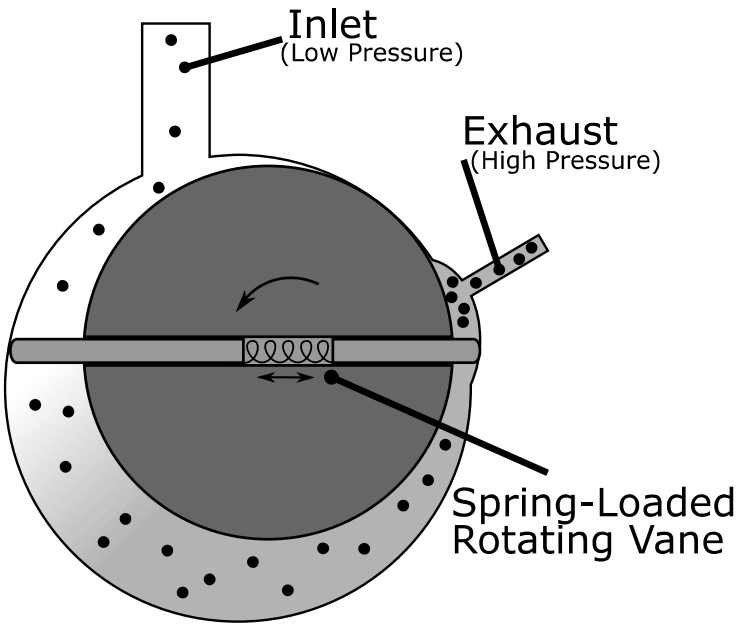

Figure 3. Rotary vane vacuum pump. This vacuum design decreases the pressure in the chamber by sealing a small volume then releasing it to the atmosphere. Two spring loaded arms are used to tightly seal the volume at all points in the pumps rotation.

In a rotary pump, particles are pushed into the inlet of the pump by pressure exerted by other particles in the chamber. Once the pressure is sufficiently decreased, the air becomes thin enough that the particles interact much less frequently and are not forced into the pump. In this case, the rotary pump becomes less useful in achieving lower pressures.

Lower pressures may be reached by using a molecular pump. A molecular pump removes individual particles by striking them and increasing their momentum in a particular direction. While these pumps are capable of reaching much lower pressures than rotary

pumps, they are often much slower or incapable of operating at atmospheric pressure [8]. These pumps are often used as a secondary pump which is engaged after a roughing pump.

The first pump of this kind, the molecular drag pump, was designed by Wolfgang Gaede in 1909 [9]. This pump, shown in Figure 4, simply pulls particles from the inlet to the exhaust by way of a rapidly rotating cylinder.

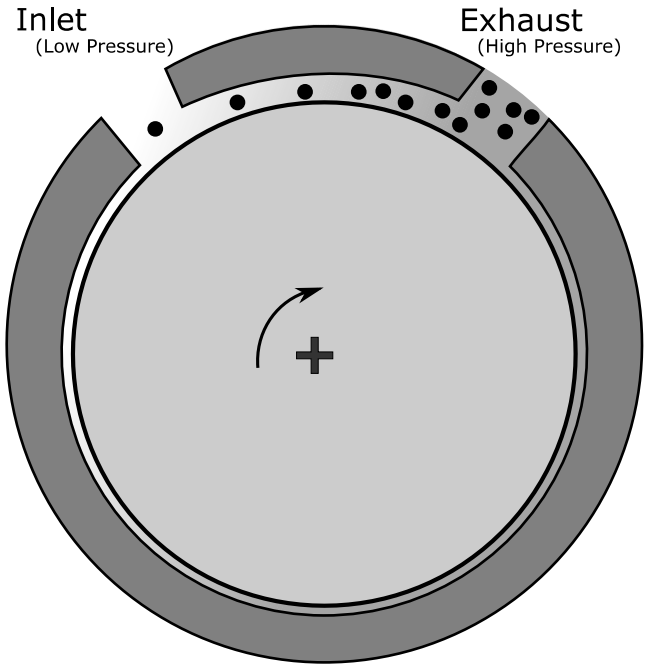

Figure 4. Molecular drag pump. This drag pump design is based on that of Wolfgang Gaede's original drag pump. The molecular drag pump spins rapidly and pulls particles to a higher-pressure area using friction. When a molecule encounters the rotating drum of the pump, the drum exerts a tangential force on the molecule, accelerating it towards the outlet. This causes more particles to travel out the exhaust of the pump, decreasing the pressure at the inlet.

Due to their theoretical functionality, molecular drag pumps must be made to very close tolerances and the clearance between the rotating mechanism and the stationary frame is only a few hundredths of a millimeter [8]. Any thermal changes or large contaminants could cause the pump to stop functioning.

Molecular drag pumps were quickly superseded by turbomolecular pumps. Turbomolecular pumps operate more efficiently than molecular drag pumps. Turbomolecular pumps, shown

in Figure 5, utilize a larger inlet as this increases the probability of a particle entering the pump. The turbomolecular pump operates on the same principle as the drag pump. However multiple layers of rotating blades add redundancy which prevents particles from returning to the chamber once they have entered the pump. This redundancy increases the allowable tolerances on the pump making them easier to manufacture and more reliable.

A well-equipped vacuum system will include a radial pump as well as a turbomolecular pump. The radial pump acts as a roughing pump, creating an area of lower pressure on the high-pressure side of the turbomolecular pump.

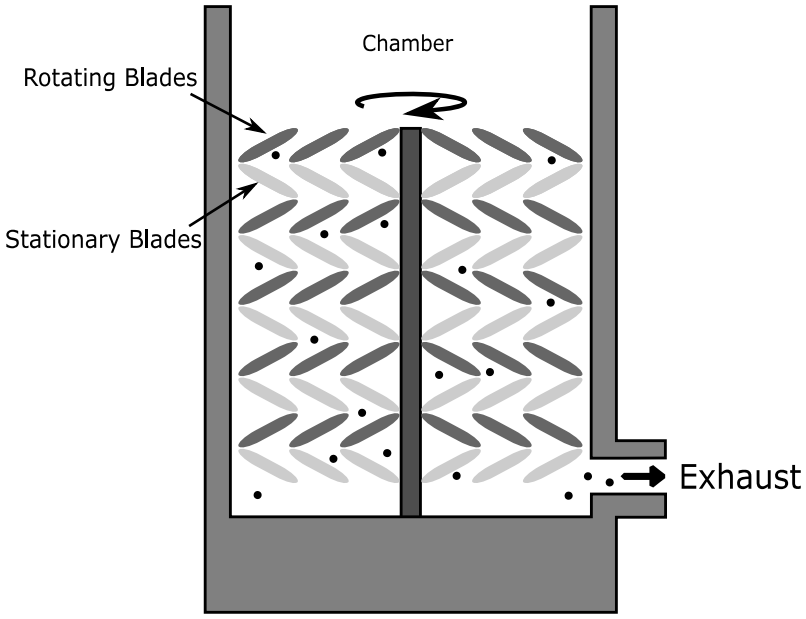

Figure 5. Turbomolecular pump. The turbomolecular pump has a wide opening at its inlet to increase the likelihood of capturing a particle. Once a particle has entered the pump, it is passed through a series of rotating and stator blades which prevent the particle from travelling back into the chamber. Once the particles reach the bottom of the pump, the pressure may build up and a rotary pump may be used to lower the pressure.

1.2.2. High Voltage

The purpose of the vacuum chamber is to facilitate thin film deposition. The material to be deposited, or target material, is placed in a crucible and heated through a process called thermionic emission. The target material is bombarded with electrons emitted by a tungsten filament and attracted towards the crucible by a high potential difference. In order to obtain

a high enough potential, the 120 V potential supplied by a wall socket must be increased to 4 kV. AC high voltage may easily be obtained through the use of a transformer. To understand the operation of the high voltage power supply, it is necessary to discuss the propagation of a magnetic field and inductance.

As current is passed through a wire, the wire produces a magnetic field. The direction of this field curves around the wire as shown in Figure 6. Ampères law gives the magnitude of the magnetic field,

$$B = \frac{\mu I}{2\pi r} \tag{1}$$

where μ is the permeability of the material through which the magnetic field is propagating, I is the current through the wire, and r is the distance from the wire. The magnitude of the magnetic field is directly related to the current through the wire and is inversely related to the distance from the wire. At a certain distance, the magnitude of the magnetic field will be stronger in a material with a higher magnetic permeability. In transformers and solenoids, wire is generally wrapped around an iron core because it has a much higher magnetic permeability than air, increasing the efficiency of the device.

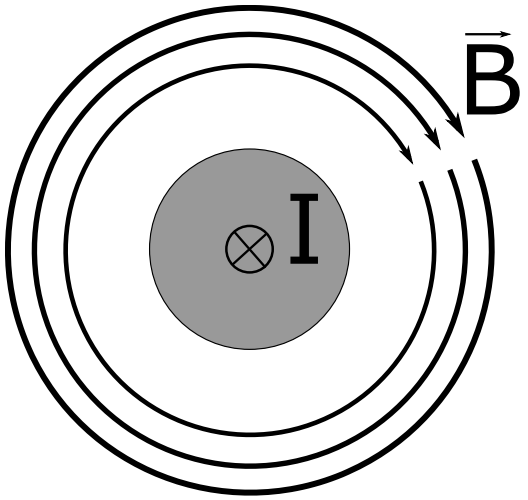

Figure 6. Magnetic field due to current in a wire. The current through the wire is into the page and induces a clockwise magnetic field which decreases radially according to Ampère's law.

Magnetic flux is defined as the integral of the magnetic field over a surface. When the current through the wire is alternating, the magnetic field alternates with the same frequency. Just as current through a wire induces a magnetic field, changes in a magnetic field can be used to induce a potential difference in a coil of wire. Faraday's law of induction defines this potential difference as

$$\Delta V = -N\frac{d\Phi_B}{dt} \tag{2}$$

where N is the number of loops immersed in a magnetic field with flux, Φ_B, that changes in time.

In a solenoid, energy is stored by inducing a magnetic field in the center of the solenoid. When a DC current is passed through a solenoid, the magnetic field increases to a constant value. If the current fluctuates, the magnetic field begins to change, inducing a potential difference that opposes the change in current. Typically, a solenoid is created with a piece of iron in the center because the magnetic permeability of iron is much higher than a vacuum. Therefore, the magnitude of the magnetic field will be larger. Figure 7 shows the magnetic field induced in a solenoid.

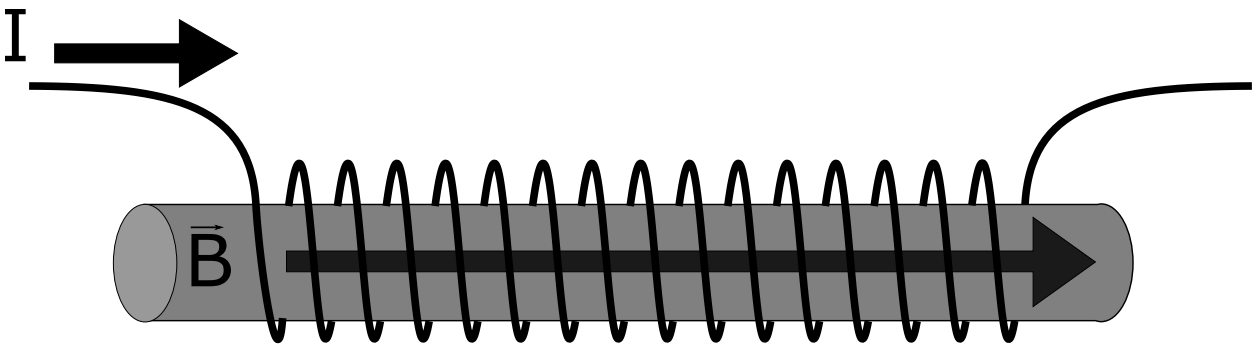

Figure 7. Magnetic field through a solenoid. Current passing through the coiled wires of a solenoid produces a magnetic field. This magnetic field stores energy and releases the energy back into the circuit as the current through the solenoid changes.

In a transformer, energy is transferred between two electrically independent coils of wire by wrapping them around the same iron core. The primary coil drives an oscillating magnetic field inducing a potential difference across each turn of wire in the secondary coil according

to Faraday's Law. The potential difference across each coil may be related to the number of windings and the magnetic flux using equation (2).

In most transformer designs, such as the one shown in Figure 8, the areas enclosed by the primary and secondary coils are equal. Because the enclosed areas are equal, the magnetic flux through each coil will be equal as long as the coils are close enough to each other that it may be safely assumed that the magnitude of the magnetic field is the same in both coils. For a transformer, equation (2) can be used to describe the potential difference across both the primary coil,

$$\Delta V_p = -N_p \frac{d\Phi_B}{dt}, \tag{3}$$

and the secondary coil,

$$\Delta V_s = -N_s \frac{d\Phi_B}{dt}, \tag{4}$$

where V represents the voltage across the coil, N is the number of wraps in the coil, and Φ_B is the magnetic flux through the coil. In a transformer, the coils are placed close together so that the magnetic field through both coils is effectively the same. The rate of change, $\frac{d\Phi_B}{dt}$, in both coils will be the same. Dividing equation (3) by equation (4) yields

$$\frac{\Delta V_p}{\Delta V_s} = \frac{N_p}{N_s} \tag{5}$$

where V_P and V_S represent the voltage in the primary and secondary coils, respectively, and N_P and N_S represent the number of turns in the primary and secondary coils, respectively. If the secondary coil has the same number of wire wraps as the primary coil, the potential across the entire coil will be the same as the primary coil. If the secondary winding has a greater number of wraps than the primary coil, then a greater voltage will be induced. Because energy must be conserved, the current that the secondary coil is capable of producing is limited by the current that the primary coil can draw from its source.

The invention of the transformer increased the feasibility of AC electricity distribution by offering a means to boost the voltage of an AC signal which has decreased in magnitude over a long wire. High voltage transformers are also used inside high voltage power supplies, microwave ovens, and medical imaging equipment.

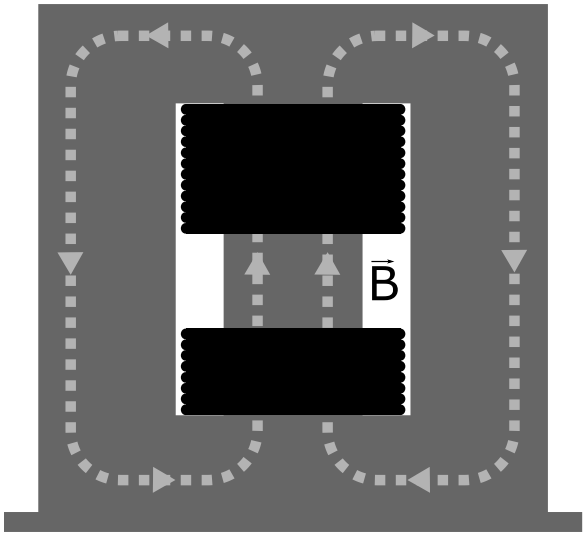

Figure 8. Diagram of a transformer. A shell type transformer used in microwave ovens contains an iron core with two electrically independent coils wrapped around its center. The primary coil produces a magnetic field which propagates through the iron core. This magnetic field induces a potential difference across each winding of the secondary coil.

1.3. Deposition Methods

1.3.1. Thermionic Emission Without Electromagnetic Alignment

The vapor pressure of a material is the pressure at which the vapor phase of a material is at equilibrium with its solid phase. The vapor pressure of a material is dependent on its temperature. Decreasing the pressure below the vapor pressure or increasing the temperature once the vapor pressure has been reached will increase the rate at which the target material evaporates.

The target material is heated by bombarding a graphite crucible with electrons. These electrons are released from a filament by thermionic emission. In order to overcome the work function of the filament, the filament is floated at a negative high voltage relative to ground. Electrons are released in all directions, but are attracted towards the relative

positive charge of the grounded crucible. Electrons strike the crucible, imparting kinetic energy, and flow to ground, creating a measurable current which may be used to quantify the power being directed to the crucible during deposition. As the temperature of the crucible is increased, thermal energy is transferred to the target material in the crucible, causing it to evaporate. As the target material is heated, the surrounding apparatus heats up as well causing built up dirt to be released into the chamber. Both heating the apparatus and evaporating the target material cause the pressure inside the chamber to rise. In this study, thin films are deposited by heating silver in a vacuum until the vapor pressure is low enough for silver to outgas.

1.3.2. Alternative Deposition Techniques

All thin film deposition processes fall into two main categories: physical processes, and chemical processes. Chemical processes are easily applied to large surfaces, and the chemicals are easily obtained [10]. Chemical deposition is used in industrial manufacturing processes because the apparatus is easily scaled to accommodate large batches of thin films. The drawback of chemical deposition is that chemical deposition offers less control over certain aspects of the deposition process and it is necessary to store and dispose of all the chemicals necessary for deposition.

Physical vapor deposition (PVD) techniques use physical methods to remove atoms from the target material and deposit them on the substrate. For example, sputtering is a PVD process where argon ions are accelerated at the target material to knock individual atoms free. These atoms are released with enough kinetic energy that they can deposit onto a substrate. Another deposition technique utilizes thermionic emission to create a focused electron beam. A hot tungsten filament is partially blocked such that a focused stream of electrons is emitted. This stream of electrons is bent and guided towards the target material using a magnetic field. The electron beam emitter must be protected from the material being deposited and it is often placed below the material and the beam is pointed horizontally. When electrons are emitted, the magnetic field guides the electrons through an arcing path to the target material. In this case, the target material is heated directly, rather than through its container.

The container is generally cooled to prevent it from introducing impurities to the film by either evaporating or mixing with the target material. While aligning the electron beam with an external magnetic field increases the quality of the deposited films, it is a less energy-efficient method of depositing a film because more energy is required to heat the target material substantially. This technique also requires more fine tuning in order to accurately align the electron beam. For large samples the electron beam is not simply focused at the center of the target, but is required to scan across the entire surface of the target in order to ensure even heating.

1.3.3. A Comparison of Deposition Techniques

In this study, thermionic emission was used to deposit a thin film of silver onto a silicon substrate. Thermionic emission was used over other PVD methods as the construction of the apparatus was more straightforward. Rather than carefully monitoring a magnetic field to guide an electron beam to the target material, the crucible is simply bombarded with electrons from below. The deposition rate of thermionic emission may be controlled by decreasing the rate of thermionic emission and allowing the silver to cool. PVD is used over chemical methods because PVD eliminates the need to store and handle large amounts of chemicals. PVD methods are widely used across the field of thin film research [11][12].

1.3.4. Feasibility

Other research groups studying the atomic structure of thin films made of gold, silver, copper, or aluminum have used thermionic emission or electron beam deposition [13][14]. Thin films of materials having a melting point higher or equal to that of silver have been deposited using electron bombardment of a graphite crucible [12][15].

Huang and Spaepen studied the tensile strength of thin films made from various materials [14]. Films were created using electron beam deposition using a base pressure of 2×10^{-7} Torr with the pressure increasing to 3×10^{-6} Torr during deposition. Films were deposited using silver, copper, and aluminum. Additionally, silver and copper were deposited in alternating layers to create multilayer films. Houghton College is attempting to deposit silver using thermionic emission within the same range of pressures as Huang and Spaepen.

1.4. Motivation for Research

1.4.1. Practical Uses of Thin Film Processes

Thin films have practical applications in a variety of fields including energy collection and storage, remote sensing, and semiconductor design [10]. Many optical systems such as lenses, mirrors, waveguides, and polarizers are made using chemical deposition processes [10]. Solar energy collection has caused an increase in the rate of thin film research [16]. Thin film based energy collecting products are becoming a reality on the consumer market, and the continued research into the structure of thin films is important for the success of these products.

Thin silicon films are used in creating transistors and microcontrollers as well as larger computer chips. While this research project is focused on silver thin films, an understanding of the effects that thermal and mechanical stresses and strains have on thin films as a whole lends understanding to the failure rate of products which utilize thin films made from other materials.

1.4.2. Silver Crystal Structure

Thin films have unique properties when compared with macroscopic pieces of the same material. Research is actively being done to study the effect of tension and heat on thin films [12][14]. Thermal and mechanical stresses contribute to the rate of failure of thin films and are areas of particular interest.

Silver atoms form a face-centered cubic (FCC) structure. In a FCC structure a cube is formed with one silver atom at each corner and at the center of each side. These cubes form a repeating structure called a crystal or a grain. Adjacent crystals oriented in the same direction will merge to form a single large crystal. In a large piece of silver, crystals may form pointing in any direction without preference.

A thin film is defined as a material whose width is significantly wider than its thickness. The geometry of the film allows the crystal growth to act two-dimensionally. Within a two-dimensional thin film, the orientation of these crystals may be described relative to the

normal vector of the substrate on which they are deposited. Grains in certain orientations relative to the substrate are in a lower energy state than others.

The orientation of a FCC structure is described by writing the components of the normal vector in terms of the basis vectors of the crystal lattice. For example, a normal vector intersecting two atoms along the same edge indicates that the crystal has formed in a (100) orientation. Figure 9 shows a FCC structure in the 100 orientation along with arrows indicating different normal vectors relative to the FCC structure. In a thin film, the crystals tend to grow in the lowest energy state, the (111) orientation. As more silver atoms are added to the film, more crystals form on the film. These crystals generally adopt the same orientation. This pattern is repeated causing the crystal to increase in size, or grow.

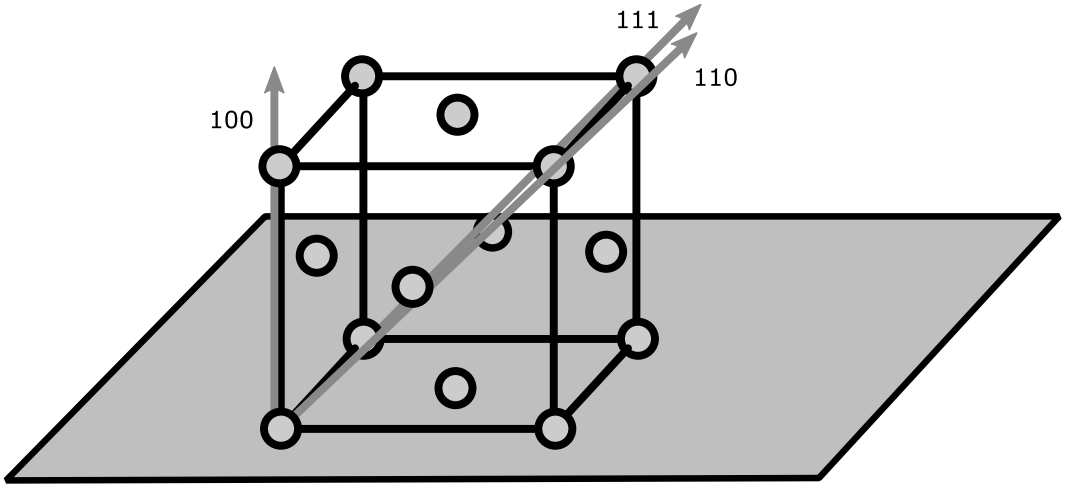

Figure 9. Face-centered cubic structure. A crystal with a face-centered cubic structure is shown in the 100 orientation with possible normal vectors for 110 and 111 orientation.

There is a small probability that crystals may form in a higher energy state. When this happens, more crystals will form in the same orientation. Over time crystals formed in a higher energy state will transform into the lower energy state. In this way, thin films are formed with crystals oriented in different directions. The texture of a film describes the amount of crystals pointed in the same direction. A highly-textured film is made up of grains which are all oriented in the same direction. Over time as grains in a higher energy state are absorbed into crystals formed at a lower energy state, the texture of the film changes.

1.4.3. Thin Film Research

Research is being done at Cornell University which studies the texture transformations of physical vapor deposited thin films [12]. Films initially deposited as (111) orientation often transform to a (100) orientation in order to minimize the energy of the film. One theory on thin film crystal structure states that transformations are caused by the interaction between the strain energy and interface energy which decreases with the thickness of the film. To verify this correlation, it is necessary to take an accurate measurement of the orientation of crystals in the film as well as the strain of the film. These measurements must be taken for films at various thicknesses.

Films were deposited using electron beam deposition and controlled using a linear shutter. The shutter was used to incrementally block a portion of the film allowing deposition to occur linearly across the substrate. This method allows films of continuously varying thickness to be deposited across the substrate while holding all other experimental variables constant. The substrate was separated by a metal strip extending parallel to the direction of motion of the linear shutter. On one side of the substrate a layer of titanium was used to offer a small amount of structural support to half of the samples. The results from this study do not follow the currently accepted model used to describe thin films, and more research must be done to develop a new model.

Other research groups have studied this phenomenon using silver and copper films deposited using evaporation and sputtering [14]. The results of these studies do not clearly show a relationship between film stresses and orientation. Baker is working to improve the consistency of deposited films including the ability to deposit films of varying thickness during a single run of the deposition process.

Work by Huang and Spaepen investigated changes in mechanical properties of thin films, specifically the relationship between yield stress and grain size. The theoretical relationship between these variables has been debated and theoretical solutions continue to disagree with experimental results. Huang and Spaepen deposit thin films made of silver, copper, and aluminum as well as silver/aluminum multilayered films. In their study, films were deposited by electron beam evaporation. The chamber was lowered to a base pressure of

$2x10^{-7}$ Torr which increased to $3x10^{-6}$ Torr during deposition. Samples were deposited to a thickness of 3 μm, determined by measuring the weight of the deposited film and assuming bulk density. X-ray diffraction revealed that the films were highly (111) textured. Once the films were deposited, they were removed from their substrate and the tensile strength of the film was measured.

Huang and Spaepen were able to record reliable data when testing the tensile strength of thin metal films. The stiffness of pure and multilayer films was approximately 20% lower than theoretical calculations. They explain that the difference in calculated and measured values is most likely due to microcracks in the thin film structure. Huang and Spaepen were able to accurately predict the relationship between yield stress and grain size for films made with large grains. The yield stress could not be accurately predicted for films made with the small grains. Theoretical models were shown to be qualitatively useful. More research is necessary to understand the numerical relationship between grain size and film strain.

Over the past 10 years, Houghton College has been working to understand the annealing process of silver thin films. Currently, Houghton College cannot deposit their own films and must rely on the resources of other research groups. A working thin film deposition chamber will allow our research team to produce our own films, modify parameters, and perform experiments more rapidly than before.

1.4.4. Viewing Thin Films

Once a film has been deposited, the structure of the film must be investigated. At Hougthon college, a variety of instruments are available for the analysis of thin films. Electron backscatter diffraction (EBSD), scanning electron microscopy (SEM), laser interferometry, and x-ray diffraction (XRD) can all be used to determine various properties of the film. The college currently has a working SEM with EBSD capability (Leica 440) and a phase-stepping laser interferometer. These may be used to view the surface of the thin film.

The goal of thin film research at Houghton College is to better understand the texture transformations of silver thin films when subjected to thermal annealing. An XRD is required to measure the amount of grains in a certain orientation within a thin film. An apparatus is

currently under construction to measure x-ray diffraction off of thin films. This apparatus will be able to determine the ratio between various orientation of crystals in a thin film.

Chapter 2

APPARATUS

2.1. Vacuum Chamber

2.1.1. Overview

The apparatus consists of a series of pumps connected to a low-pressure chamber. Once the chamber has been evacuated, thermionic emission is used to heat a crucible containing the target material. The material is heated until it begins to degas. A rate monitor is under development to predict the thickness of films as they are deposited.

2.1.2. Design

The vacuum chamber is an aluminum cylinder 91 cm (36 in) long and 28 cm (11 in) in diameter, as shown in Figure 10. It features multiple mechanical and electric feedthroughs along the sides and top of the chamber. Viewing ports are located on the bottom of the chamber directly below the substrate and on the side. These are useful for determining when the silver has fully melted and whether arcing is occurring near the crucible. The chamber is sealed with Viton o-rings, and the pressure is lowered using a rough pump (Alcatel 2004a) and a turbo molecular pump (Pfeiffer Balzers TPU-060).

The physical feedthroughs are not currently in use, but are designed for future applications. The substrate is mounted on a rotary feedthrough so that the sample may be rotated during deposition. An electrical feedthrough is also located near the substrate so that the sample may be heated using thermoelectric heating. A linear feedthrough is mounted such that the substrate may be incrementally blocked to create films of varying thicknesses or to block the substrate altogether. A rotary feedthrough is also located on the side of the chamber near the crucible. A shutter may be mounted here to cover the crucible while it is heating. Once the target material begins to degas, the shutter may be rotated away from the crucible to begin deposition onto the substrate.

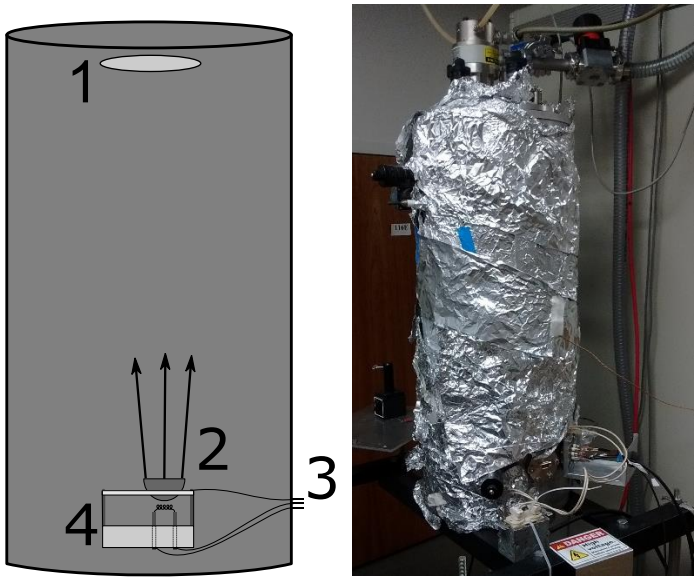

Figure 10. Mechanical diagram and image of deposition chamber. A mechanical drawing of the chamber (left) featuring the silicon substrate (1), crucible (2), electrical feedthroughs (3), and deposition block (4). An image of the chamber (right) showing the electrical feedthrough and turbo pump. The chamber is wrapped in aluminum foil to distribute heat from the resistive heating element.

The crucible and filament are mounted on a ceramic block, called the deposition block. The crucible is suspended above the filament. The design of the crucible holder has changed multiple times. The first design for the crucible holder was a piece of ceramic similar in size to the deposition block with four holes to facilitate the deposition of multiple materials. This design failed because the ceramic was not able to effectively distribute heat away from the crucible and the ceramic cracked. The second design held the crucible above the filament using a steel plate. The steel was able to distribute the heat without being damaged. This design also added an aluminum radiation shield designed to reflect more emitted electrons towards the crucible. The radiation shield absorbed enough infrared radiation that the surface began to melt. Once the radiation shield became rough it was not able to effectively reflect electrons towards the crucible. The third design attempted to move as many structural elements away from the filament as possible. A molybdenum rod was bent into a hook to hold the crucible. The thermal transmission coefficient of heat through molybdenum is much higher than steel, and the target material was not effectively heated. The final design

is simply the second, steel design with the aluminum radiation shield removed. An image of each of these four designs is shown in Figure 11.

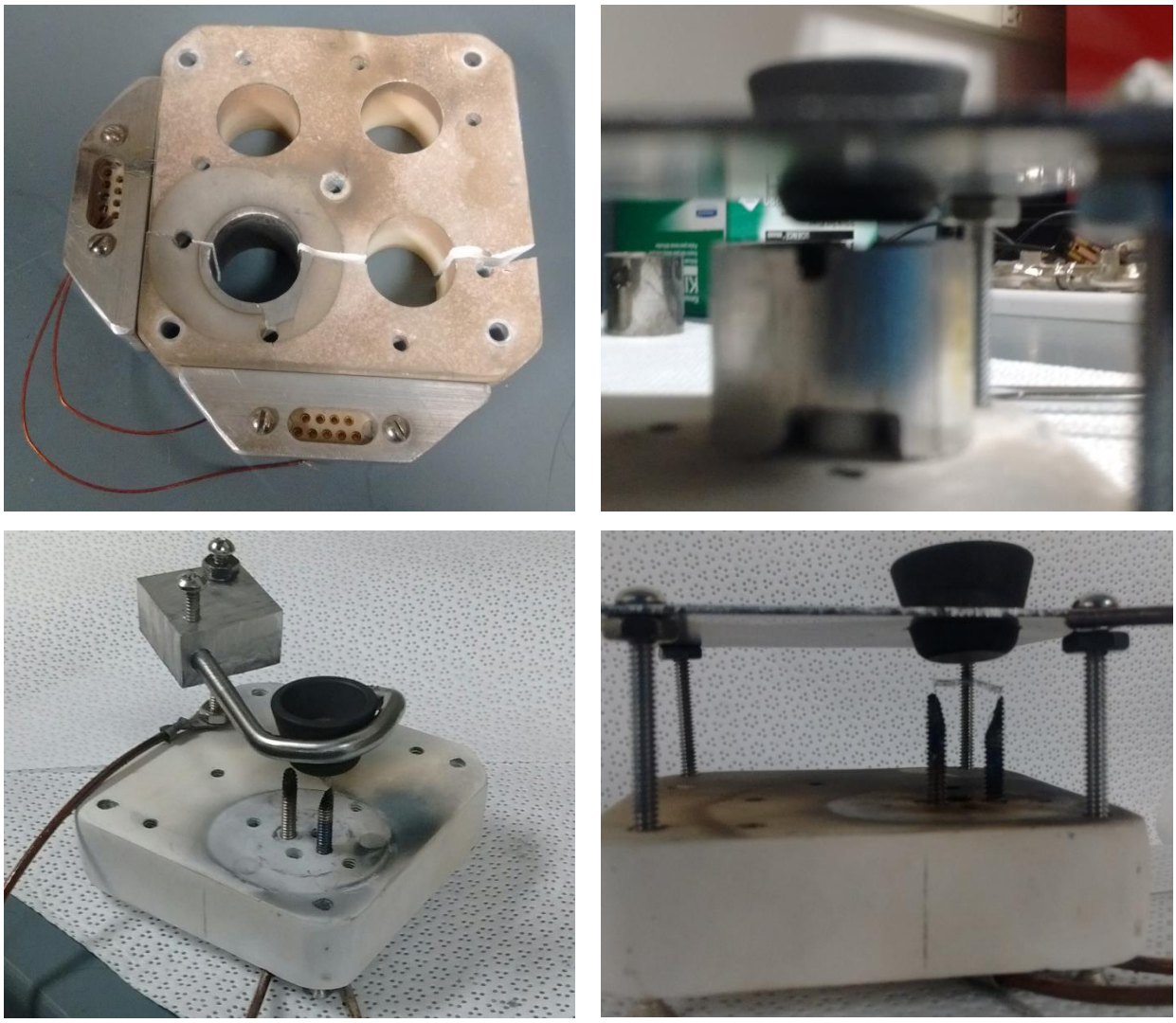

Figure 11. Images of various crucible holder designs. Ceramic block (top left), steel plate with radiation shield (top right), molybdenum rod (bottom left), steel plate without radiation shield (bottom right). Designs are listed in chronological order.

The filament posts travel all the way through the deposition block. When the radiation shield was added, the electrical connections to the filament posts were moved from the top of the deposition block to the bottom to avoid shorting the filament voltage through the radiation shield. The deposition block must now be elevated above the bottom of the chamber to avoid shorting either the filament voltage or the high voltage potential at which the filament is

floating. This is accomplished threading four screws into the bottom of the block as shown in Figure 12.

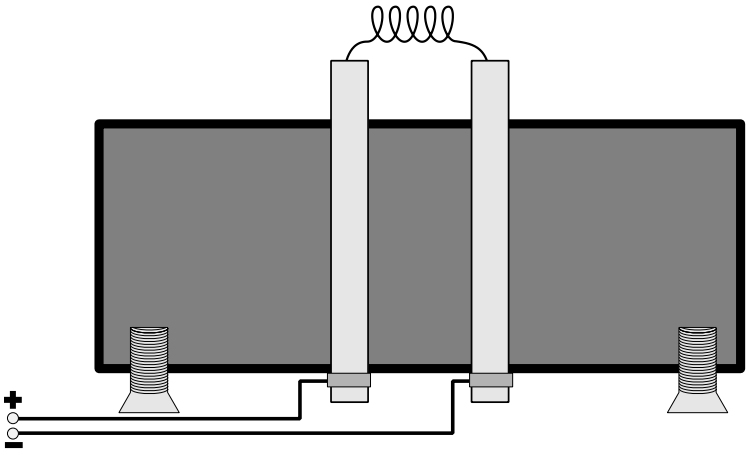

Figure 12. Diagram of deposition block. Conductive filament posts travel through the body of the ceramic deposition block. These are connected to a positive and negative DC voltage which powers the filament. Steel screws are used to elevate the block so the posts remain electrically isolated from the grounded chamber.

2.2. Circuit

2.2.1. Original Transformer

The original circuit design utilized a single high voltage transformer (Elscint 8536) controlled by a variable AC power supply. The transformer output 5 kV which was rectified using a bridge rectifier and smoothed with a capacitor as shown in Figure 13. The positive output was tied to ground and the negative output was used to float the filament. Multiple thin silver films were deposited using this method, but the voltage and the current were out of phase, causing the circuit to have a lower power factor and perform inefficiently. After a year of operation, the transformer used in this circuit was not able to produce the desired voltage and current and had to be retired.

2.2.2. Microwave Transformers

When designing the new circuit, the requirements of the power supply were reevaluated so that other designs may be considered. The circuit must be able to produce high voltage between 3-5 kV while maintaining a steady output current of 100 mA. The parts must be readily available in the lab or easily obtainable on a low budget. The circuit contained within

an off-the-shelf microwave meets these requirements. Using a single microwave circuit produces a half-rectified wave. A second transformer was used to produce a fully-rectified AC output.

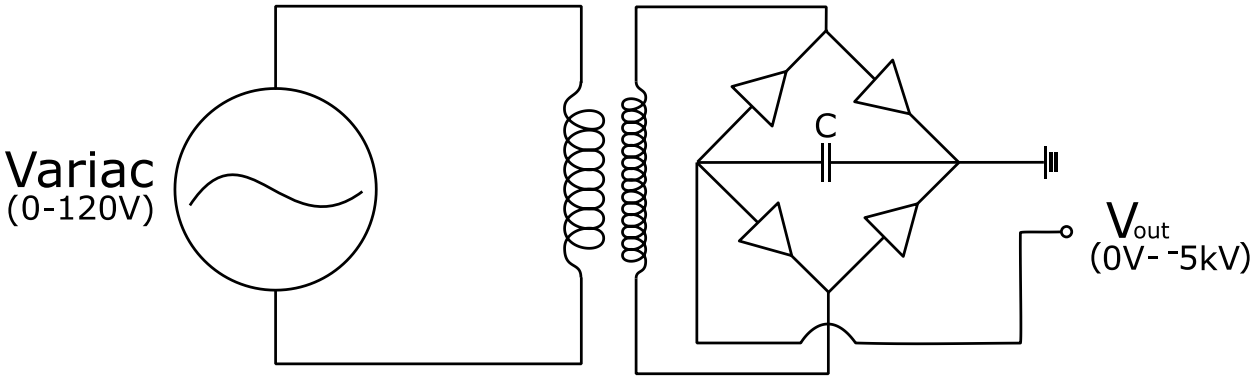

Figure 13. Original circuit diagram. A manually adjustable AC power supply drove a high voltage transformer coil. The voltage was increased to high voltage, rectified using a bridge rectifier and smoothed via a 29 nF capacitor, C1. The positive output of the bridge rectifier was shorted to ground, and the negative end was connected to the filament.

The circuit, shown in Figure 14, was redesigned and built using low-cost microwave transformers (OBJY2) obtained from eBay, and high voltage capacitors and diodes purchased from Digikey. The new design, rather than relying on a bridge rectifier and a single high voltage transformer, utilizes two 1.5 μF capacitors, C_2 in Figure 14, and four high voltage diodes to simultaneously double and rectify the output voltage of two microwave transformers out of phase. It is possible to smooth the output by adding a high-voltage capacitor between Vout and ground, increasing the power delivered to the crucible. This is not necessary as enough power is already delivered to the crucible to melt silver. This capacitor may be added in the future to deposit materials with a higher melting point. When the output of the power supply is at its peak, the filament emits electrons to the crucible. Using two microwave oven transformers out of phase doubles the frequency of the output voltage. While one transformer delivers power to the crucible, the other transformer charges its capacitor. A diode ensures that whichever transformer is outputting a lower voltage is delivering electrons to the crucible.

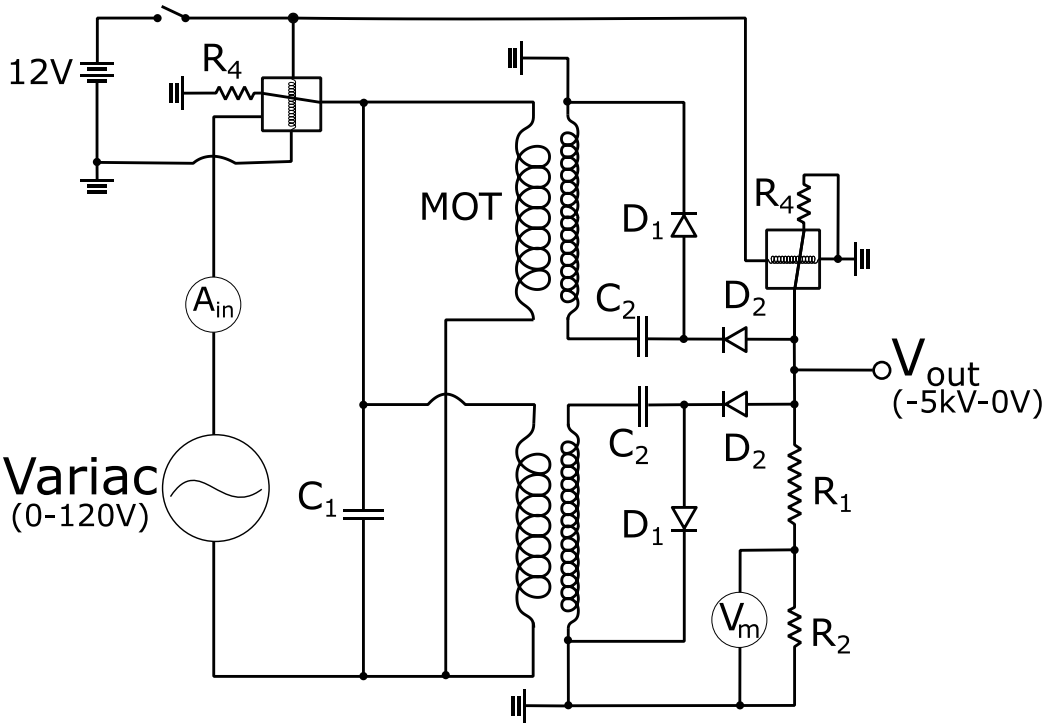

Figure 14. Updated circuit diagram. The original transformer is replaced with two smaller microwave oven transformers (MOT). The output of these transformers is doubled and rectified, but not smoothed. The 49 μF capacitor C_1 corrects the power factor of the two transformers. The two 1.5 μF capacitors, C_2, and diodes labeled D_1 are used to double the output voltage. The two diodes labeled D_2 connect V_{out} to the R_1 (40 MΩ) and R_2 (10 MΩ) form a voltage divider to measure the output voltage. V_m is measured with an oscilloscope probe utilizing an internal voltage divider. V_m is V_{out} / 50. The variac is connected to the circuit, and the output is disconnected from ground by two interlocked relays controlled by a DC power supply.

The output of each transformer is half-rectified and doubled. Because the output of the transformer is not smoothed, the output signal is not a pure AC or DC signal. Instead it is a negative, fully rectified, sine wave with an amplitude of 2 kV, at a negative DC offset of 2 kV. The output of both transformers is shown in Figure 15. The output of the power supply, shown in Figure 16, is always connected to whichever transformer is producing a lower potential by a diode. The output of the supply may be smoothed to a DC output by adding a high voltage capacitor between the output and ground. This would increase the power output of the circuit and may be necessary to deposit materials with a higher melting point.

The power supply is capable of delivering enough power to melt silver, and a smoothing capacitor has not been added.

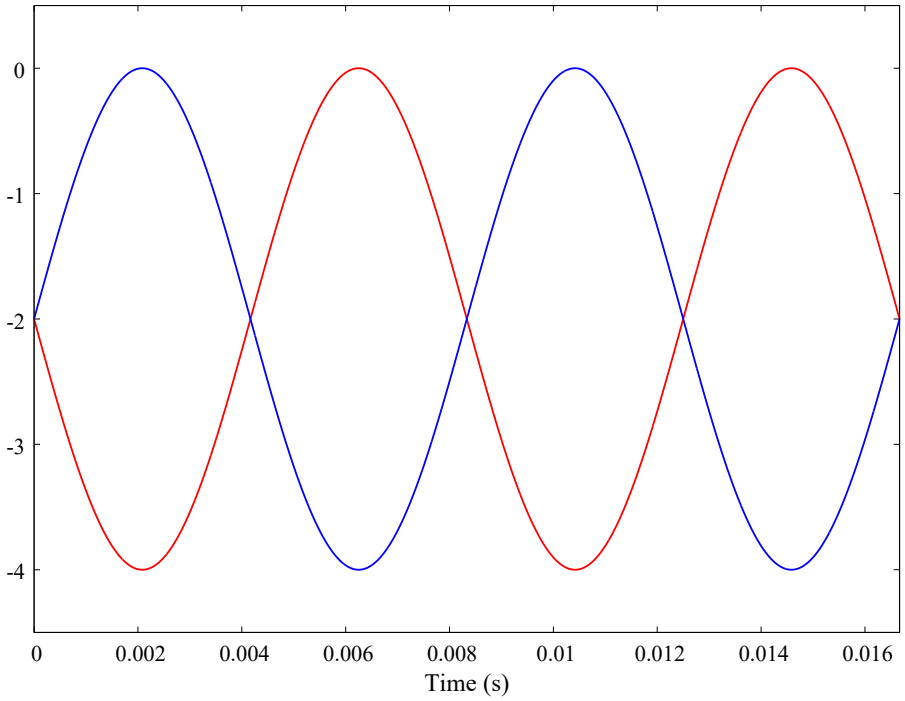

Figure 15. Computer simulation of transformer output. Two transformers (red and blue) are out of phase by 180°. Each transformer is connected to the output by a diode. These diodes select which transformer is producing the lowest potential and connect it to the output.

2.2.3. Power Factor

In a circuit with inductive or capacitive components, the relative phase of the voltage and current will be shifted. This phase shift is related to the impedance of the circuit, and may be changed by adding components with a complex impedance. In the case of a transformer, the inductive load will cause the voltage to lag behind the current. A capacitive load may be added as shown in Figure 17 to shift the phase of the voltage forward in time.

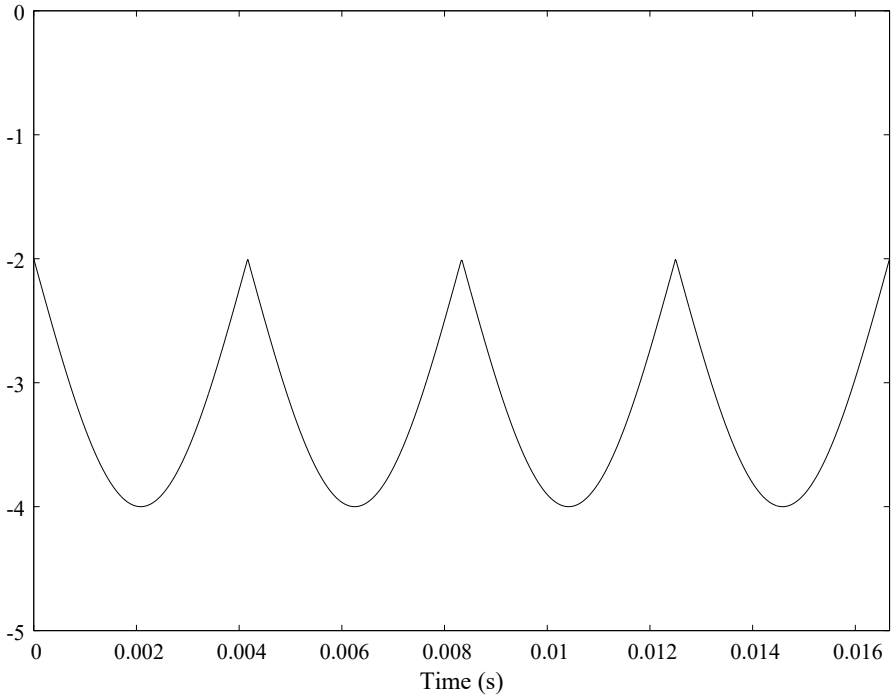

Figure 16. Computer simulation of power supply output. The output of the power supply is a centered at -2 kV, and fully rectified on the negative side. This output could be smoothed by adding a high voltage capacitor to the output.

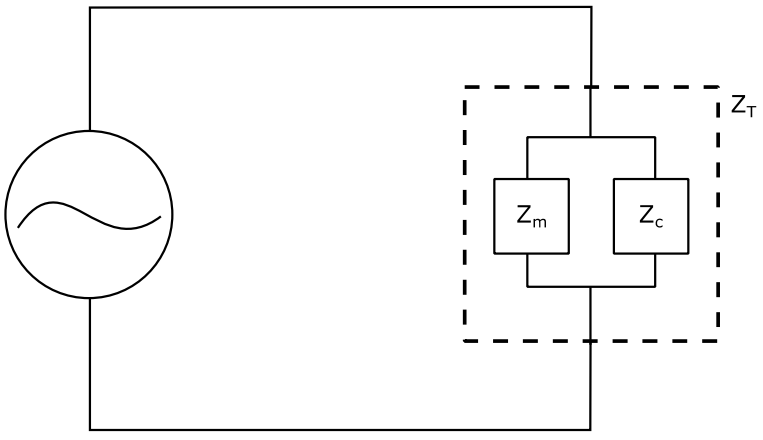

Figure 17. Impedance of the circuit. The phase shift induced by the measured impedance, Z_m, may be changed by adding a capacitor. The total impedance is related to the existing impedance from the transformers and the additional capacitive impedance, Z_C.

In general, the impedance of a component may be found using

$$\boldsymbol{Z}_m = \frac{\boldsymbol{V}}{\boldsymbol{I}} \tag{6}$$

where $\boldsymbol{V}$ and $\boldsymbol{I}$ fully describe the voltage and current including a phase shift. $\boldsymbol{V}$ and $\boldsymbol{I}$ may be written as

$$\boldsymbol{V} = ve^{i\theta_1}, \tag{7}$$

where v is the amplitude of the voltage, and

$$\boldsymbol{I} = Ie^{i\theta_2}. \tag{8}$$

where I is the amplitude of the current and θ_1 and θ_2 are the phase angles of voltage and current, respectively. The exponential forms of $\boldsymbol{V}$ and $\boldsymbol{I}$ may be combined and written in terms of sine and cosine. In general, the impedance of a component may be written in terms of the amplitudes of $\boldsymbol{V}$ and $\boldsymbol{I}$ as well as the phase shift as

$$Z_m = \frac{\mathrm{V}}{\mathrm{I}}(\cos\phi + i \cdot \sin\phi), \tag{9}$$

where ϕ is the phase difference between θ_1 and θ_2. Given the impedance of a capacitor,

$$Z_C = \frac{1}{i\omega C}, \tag{10}$$

the total impedance may be written as

$$Z_T = \frac{1}{\frac{1}{Z_m} + \frac{1}{Z_C}} = \frac{1}{\frac{I}{V} \cdot \frac{1}{(\cos\phi + i \cdot \sin\phi)} + i\omega C}. \tag{11}$$

This may be simplified and rewritten by multiplying the numerator and denominator of $Z_m$by $\cos(\phi) + i\sin(\phi)$. Finally, the total impedance may be written as

$$Z_T = \frac{1}{\frac{I}{V}(\cos\phi - i \cdot \sin\phi) + i\omega C}. \tag{12}$$

As the phase difference between voltage and current decreases, the imaginary portion of Z_T decreases. The value of the capacitor that maximizes the power factor may be found by

solving for the capacitance when the impedance is real. The expression for this capacitance is given by

$$C = \frac{I \cdot \sin\phi}{V\omega}. \tag{13}$$

Because these values were found using measurements with some uncertainty, we must know the capacitance with some uncertainty. The uncertainty in ω is relatively small in comparison to the uncertainty of V, I, and ϕ. The uncertainty of the capacitance,

$$\delta C^2 = \delta V^2 \left(\frac{\partial \mathrm{C}}{\partial \mathrm{V}}\right)^2 + \delta \mathrm{I}^2 \left(\frac{\partial \mathrm{C}}{\partial \mathrm{I}}\right)^2 + \delta \phi^2 \left(\frac{\partial \mathrm{C}}{\partial \phi}\right), \tag{14}$$

may be found by propagating the error of equation (13).

2.2.4. Safety Shutoff

For the safety of the students operating the apparatus, it is necessary to shut off the input voltage when a door is opened into the high voltage chamber. In the final design, two relays are used to disconnect the input power from the variable AC voltage supply and discharge all capacitors. These relays are controlled by an interlocked 15 V power supply. When either of the doors enclosing the high voltage circuitry are open, this power supply is disconnected from the control pin on each relay. The input power is disconnected and any power stored in the capacitors is drained through a 1 Ω, 200 W resistor. The time constant for this RC circuit is on the order of microseconds, and the circuit quickly becomes safe.

Chapter 3

RESULTS

3.1. Power Factor Measurements

The power may be found from the phase difference between voltage and current. This phase shift was measured by observing the phase of the voltage and current using the circuit shown in Figure 18.

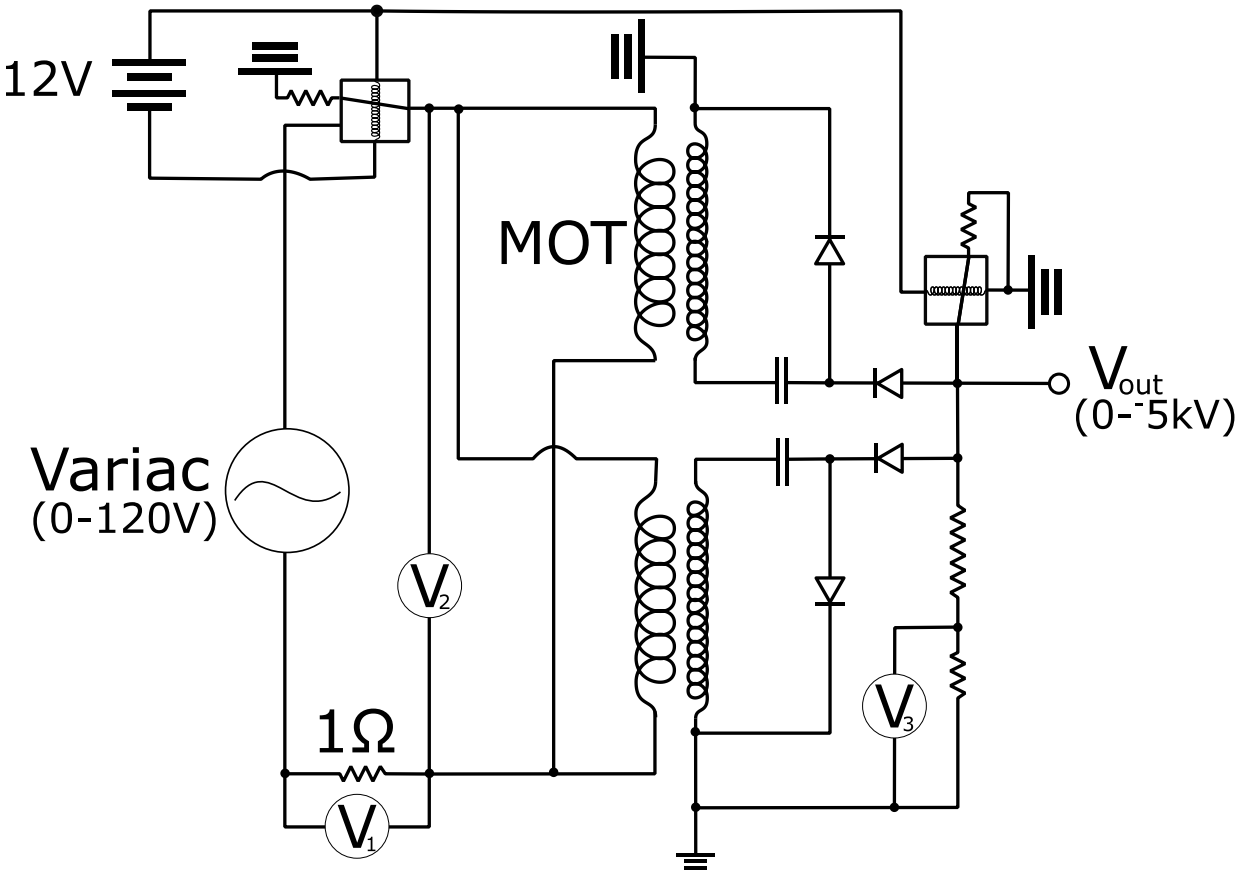

Figure 18. Updated circuit diagram for determining phase difference. An oscilloscope was used to determine the phase of the voltage and the current being sourced from the variac. The voltage measured at V_1 across the 1 Ω resistor is equivalent to the current through the variac. The voltages measured at V_2 and V_3 are the voltage output by the variac and 1/10 the high voltage output, respectively.

The current from the variac was determined by measuring the voltage across a 1 Ω resistor placed on the grounded side of the variac output. By Ohm's law,

$$V = IR, \tag{15}$$

the voltage and current across a 1 Ω resistor are equal. This voltage was measured directly using an oscilloscope. The voltage output by the variac was measured using an oscilloscope lead and a voltage divider, which reduced the voltage by a factor of 10.

The voltages and current were shown in real time on the display of an oscilloscope and saved to a USB memory stick. In order to maximize the power factor, the voltage and the current should be in phase. The phase shift was determined by measuring the time difference between the maximum value of voltage and current visually on an oscilloscope. The impedance of the circuit was calculated from the measured phase shift as shown in (6). The input voltage and current were measured to be 60 V and 1.2 A using an oscilloscope. A phase shift of 1.2 radians was measured between the current and the voltage by measuring the distance between peaks on the display of the oscilloscope, dividing by the length of one period, and multiplying by 2π. Assuming a relatively large uncertainty of ±1 V, ±0.3 A, and 0.2 radians, we find a capacitor value of 49 μF ± 13.0 μF. Measurements were also taken with an input of 95 V and 2 A suggesting a capacitor value of 52 μF ± 8.8 μF. A 49 μF capacitor was added in parallel with the transformers, and the phase difference remeasured. The initial and final phase difference may be seen in Figure 19.

3.2. Thin Film Deposition

Multiple attempts were made towards depositing a thin film. While the silver was heated to a red glow on multiple occasions, deposition has not yet been acheived. Every aspect of the deposition system must be operating properly for a film to be deposited. The most important factors when attempting to deposit a film are the maximum power the power supply can deliver, the design of the crucible holder, and the base pressure of the chamber.

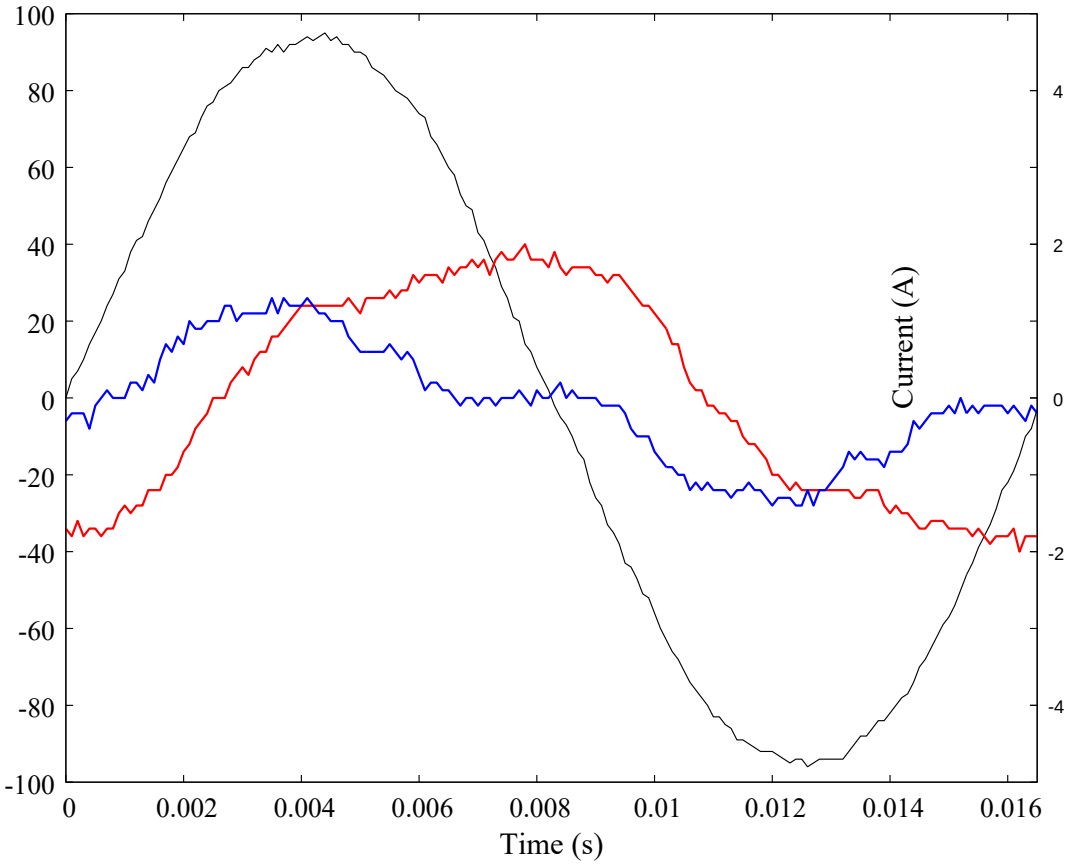

Figure 19. Phase difference measurements. Input voltage (black, left vertical axis) vs. time. Input current before power factor correction (red, right vertical axis) and after the phase was corrected (blue, right vertical axis).

During the first attempt at deposition, the chamber was clean and the base pressure was approximately $5x10^{-7}$ Torr. A film could not be deposited because the high voltage transformer was not capable of supplying the necessary power to the circuit. To improve the power supply, the circuit was redesigned according to the circuit shown in Figure 14. This power supply is capable of delivering enough power to melt silver.

Once the power supply was updated to supply the necessary power, the deposition block needed to be modified. The silver was not heating up enough to deposit a film. The steel plate was replaced with a curved molybdenum rod. Molybdenum has a high coefficient of thermal conductivity and heat was drawn away from the crucible before the silver was able to melt. During a test of this design, that the power supply was capable of delivering 400 W of power to the crucible. Previous deposition experiments performed at Houghton College have noted

that silver can melt when the filament is drawing 300 W from the power supply. During this trial, the heat was distributed across the molybdenum arm and the silver did not melt.

The original design of the crucible holder was used again, but without the aluminum radiation shield. This design has not been fully tested yet because the base pressure in the chamber is $5x10^{-6}$ Torr after baking. While this is a good deposition pressure, the pressure will rise significantly once the filament is powered and the silver begins to degas. It appears there is either a leak in the chamber or there is a poor seal around the opening. This could be caused by either a misaligned or damaged O-ring.

Chapter 4

CONCLUSION

4.1. Present State of the Instrument

4.1.1. Power Supply

The power supply is capable of supplying fully-rectified, negative, high voltage power to the filament. This output is not smoothed. However, a high voltage capacitor may be placed between the output of the power supply and ground to store charge during the off-cycle phase of the transformer. The safety shut off in place will drain this capacitor when the safety power supply is turned off.

The electrical feedthrough is rated for 5 kV. However, arcing was noticed during multiple tests at incrementally lower voltages. One of the high voltage connections was not able to withstand the high voltage anymore and was leaking current to the grounded chamber. This has been rectified for the time being by using a different pin. The feedthrough will need to be replaced in the future.

4.1.2. Deposition Block Design

The design of the deposition block has changed many times over the course of this experiment. The current design suspends the crucible above the filament by a steel plate without attempting to increase the number of electrons emitted towards the crucible through the use of a radiation shield. This design has not been thoroughly tested due to trouble reducing the pressure in the chamber.

4.2. Future Work

4.2.1. Rate Monitor

In the future, we would like to be able to measure the rate at which deposition occurs in the chamber to predict the thickness of the film we are depositing. A rate monitor measures the amount of conductive metal ions travelling through the chamber and determines the rate at which it is being deposited. Measuring this rate is important for fine tuning the deposition process and being able to accurately deposit films of a particular thickness.

Ion gauges have been used to measure pressure. In this application, the current reading from the ion guage correlates not only to the pressure within the chamber, but also to the rate of deposition [17]. Electrons are emitted from a tungsten filament. These electrons ionize atoms of the target material which are then accelerated towards the collector by the anode. As atoms of the target material are deposited on the collector they regain their electrons generating a current. This current may be measured and correlated with the rate at which the target material is being deposited.

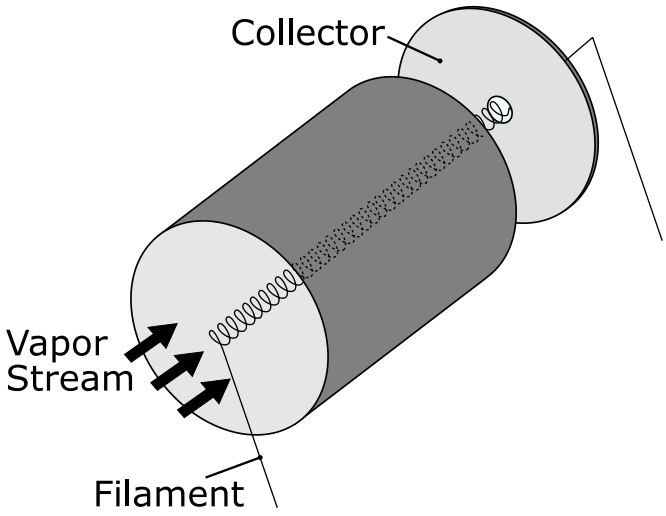

Figure 20. Rate monitor. Atoms of the target material are ionized and accelerated toward the collector. As target ions are deposited on the collector, they regain electrons generating a measurable current. This current correlates with pressure and may be used to determine the deposition rate.

4.2.2. Temperature Controlled Deposition Target

After a film has been deposited, the silver atoms form crystals in various orientations. As silver is deposited, the crystals on the substrate begin to grow, maintaining their orientation. Crystals increase in size until they encounter other crystals growing on the film. After deposition, adjacent crystals will begin to anneal, gradually taking on the crystal orientation of adjacent crystals if they are of a lower energy. This process may be expedited by heating the sample.

Appendix A Preparing the Chamber

In order to deposit a thin film, the pressure in the chamber must be low enough for the filament to operate without breaking. Lower pressures are also necessary to deposit pure films. $1x10^{-7}$ Torr is a good base pressure for depositing a film. Lowering the pressure to this level is an iterative process which may take more than a week depending on the state of the chamber and the quality of the air in the laboratory. Opening the chamber to a humid laboratory will increase the amount of time required to lower the pressure.

While working on parts for the deposition chamber it is important to work on a clean area and wear gloves to prevent oils from building up on the parts. Any water or oil in the chamber will degas, increasing the time it takes to lower the pressure. For this reason, it is also important to maintain a low humidity in the lab and if the chamber will not be operated for a long period of time, it should be kept at vacuum or, at the very least, sealed.

After the chamber has been sealed entirely, the rough pump should be turned on and the pressure in the tube leading to the chamber lowered. The pressure in this tube should always be below atmospheric pressure whenever the chamber is open to prevent machine oil from the rough pump from leaking backwards into the turbo pump and the chamber. Once the pump is on, the valve to the chamber may be opened and the pressure should be brought down to the low 10^{-2} Torr range.

Once the pressure falls below $5x10^{-2}$ Torr, the turbo pump may be turned on. Initially the pump will run loudly, increasing in volume until it reaches its resonant frequency. As the speed of the turbo increases beyond this point, the pitch emitted by the turbo will suddenly increase. Depending on the conditions of the chamber, the turbo should lower the pressure to $1x10^{-4}$ Torr within an hour. Once the pressure drops below this point, it should not be raised above $1x10^{-4}$ again while the turbo pump is running.

While lowering the pressure in the chamber it is helpful to heat the chamber using a resistive heater. This removes water vapor from the O-rings and sides of the chamber. Powering the

filament and high voltage help clean off the filament, crucible, and surrounding apparatus, further lowering the pressure and keeping the pressure lower while a film is being deposited.

The time necessary for each step of this process will vary based on the conditions of the chamber, the parts and the laboratory. New parts must be cleaned thoroughly, but will usually take some time to degas before the pressure will drop. Starting with humid air will slow the process down. Introducing a dehumidifier to the lab and using air conditioning during humid summer weather will decrease the time necessary to lower the pressure in the chamber.

Appendix B Vacuum Material Requirements

Certain materials may not be used within the vacuum chamber because their presence has a negative effect on the pressure in the chamber. The presence of organic material, plastics, and many adhesives within the chamber will prevent the pressure in the chamber from decreasing beyond a certain point. In the case of organic materials, these substances contain a high percentage of water and natural oils which release vapor under low pressures. Most plastics and adhesives give off fumes when exposed to vacuum pressures and will continue to degas indefinitely.

Due to the outgassing properties of plastics and adhesives, instruments created for use within a vacuum are generally made from either aluminum or steel, for parts which must conduct electricity, or ceramic, for parts acting as insulators. Pieces are fixed together using either steel or ceramic nuts and bolts. Care must be taken when creating instruments with a combination of ceramic and metal because ceramic is brittle and tapped holes can easily become stripped.

Appendix C Pressure Requirements

If the cold pressure of the chamber is consistently below $5x10^{-7}$ Torr, the pressure is low enough to begin deposition. When depositing a film, the temperature of the filament and crucible rise causing the pressure in the chamber to increase. While depositing, the pressure

in the chamber may rise up to an order of magnitude depending on how clean the crucible and filament are. These may be cleaned off by running the filament periodically while the chamber is pumping down. The pressure must be monitored during deposition to prevent the pressure from increasing too rapidly. Both the pressure gauge and the turbo pump are delicate instruments which should only be operated below 10^{-4} Torr.

Appendix D Depositing a Film

Once the pressure in the chamber has stabilized, a film may be deposited. During the deposition process, the crucible and surrounding structural elements of the apparatus will be heated, increasing the pressure in the chamber. To increase the longevity of the filament as well as the turbo pump, this pressure should never be allowed to rise above $1x10^{-4}$ Torr.

The controllable variables which affect the deposition process are the temperature of the chamber, filament current, and voltage at which the filament is floated. The temperature of the chamber should be as low as possible, presumably room temperature. If the chamber was heated while lowering the pressure, it should be allowed to cool. The filament current must be set before the high voltage power supply is powered. A good starting value for the filament current is 2 A. The emissions current is correlated with the filament current, voltage at which the filament as floated, and the distance between the filament and the crucible.

Interlocked doors to the high voltage chamber should be closed and the oscilloscope should be turned on prior to turning on the variac. The variac voltage should be slowly increased to approximately 10V. The oscilloscope should trigger on this input voltage. Next the safety power supply may be increased to 12 V to switch the relays, ungrounding both microwave transformers and connecting their inputs to the output of the variac. At this point the high voltage will be proportional to the voltage output by the variac. Slowly increase the high voltage to 4 kV, checking the filament current, emissions current, and pressure in the chamber regularly.

R e f e r e n c e s

[1] A. Wolf, A history of science, technology, and philosophy in the 16th & 17th centuries (George Allen & Unwin, London, 1968).
[2] E. Torricelli, *Letter to Michelangelo Ricci concerning the barometer (1644).*
[3] Sprengel, *Researches on the Vacuum* (1865).
[4] O. von Guericke, *Experimenta Nova* (1672).
[5] *Reports by the Juries on the Subjects in the Thirty Classes Into which the Exhibition was Divided* (William Clowes and Stamford Street and Charing Cross, 1852).
[6] E.C. Andrade, Vacuum **9**, 41 (1959).
[7] P.A. Redhead, in *CERN Accelerator School Vacuum Technology*, edited by S. Turner (CERN, Geneva, Switzerland, 1999), pp. 281-290.
[8] D.M. Hoffman, B. Singh, and J.H. Thomas, *Handbook of vacuum science and technology* (Academic Press, San Diego, CA, 1998).
[9] W. Gaede, 1069408 (1913).
[10] R. Mane, Mater. Chem. Phys. **65**, 1 (1999).
[11] E. Klokholm, J. Electrochem. Soc. **115**, 8 (1968).
[12] S. P. Baker, B. Hoffman, L. Timian, A. Silvernail and E. A. Ellis, Acta Mater. **61** 19 (2013).
[13] A. Folch, J. Tejada, C. H. Peters and M. S. Wrighton, Appl. Phys. Lett. **66**, 16 (1995).
[14] H. Huang, Acta Mater. **48**, 12 (2000).
[15] H. O'Bryan, Rev. Sci. Instrum. **5**, 3 (1934).
[16] A. G. Aberle, Thin Solid Films **517**, 17 (2009).
[17] G. Giedd, Rev. Sci. Instrum. **31**, 7 (1960)